

Thickness dependence of the magnetic properties of barium ferrite films prepared by pulsed laser deposition

Chengbo Zhao(赵诚博), Bowei Han(韩博纬), Yuchen Zhao(赵宇辰), Yang Sun(孙洋), Lichen Wang(王利晨), Ruoshui Liu(刘若水), Yunzhong Chen(陈允忠), and Dengjing Wang(王登京)
Citation: Chin. Phys. B, 2026, 35 (**2**): 027504. DOI: 10.1088/1674-1056/adf6a5
http://cpb.iphy.ac.cn; http://iopscience.iop.org/cpb

What follows is a list of articles you may be interested in

Temperature and angle dependence of magnetic damping in manganite thin films

Jinghua Ren(任京华), Yuelin Zhang(张跃林), Miming Cai(蔡米铭), Yuhan Li(李语涵), Mingming Li(李明明), Tianqi Wang(王天琦), Dekun Shen(沈德坤), Hongyu Zhou(周鸿渝), Xiangwei Zhu(朱祥维), and Jinxing Zhang(张金星)
Chin. Phys. B, 2025, 34 (**10**): 107504. DOI: 10.1088/1674-1056/ade06d

Direct observation of ultrafast magnetization dynamics in Co/Ni bit patterned media by time-resolved scanning Kerr microscopy

Wei Zhang(张伟), Wei He(何为), Qin-Li Lv(吕琴丽), Jian-Wang Cai(蔡建旺), Xiang-Qun Zhang(张向群), and Zhao-Hua Cheng(成昭华)
Chin. Phys. B, 2025, 34 (**4**): 047501. DOI: 10.1088/1674-1056/adb67e

Perpendicular magnetic anisotropy of Pd/Co_2MnSi/Co/Pd multilayer

Xiaoqi Qin(秦晓奇), Jiaxing Tan(谭家兴), Xianwu Xiu(修显武), Wentian Cao(曹文田), and Shuyun Wang(王书运)
Chin. Phys. B, 2025, 34 (**3**): 037502. DOI: 10.1088/1674-1056/ada694

Low Gilbert damping in Bi/In-doped YIG thin films with giant Faraday effect

Jin Zhan(湛劲), Yi Wang(王一), Xianjie Wang(王先杰), Hanxu Zhang(张晗旭), Senyin Zhu(朱森寅), Lingli Zhang(张伶莉), Lingling Tao(陶玲玲), Yu Sui(隋郁), Wenqing He(何文卿), Caihua Wan(万蔡华), Xiufeng Han(韩秀峰), V. I. Belotelov, and Bo Song(宋波)
Chin. Phys. B, 2024, 33 (**10**): 107505. DOI: 10.1088/1674-1056/ad6b84

Bismuth doping enhanced tunability of strain-controlled magnetic anisotropy in epitaxial $Y_3Fe_5O_{12}$(111) films

Yunpeng Jia(贾云鹏), Zhengguo Liang(梁正国), Haolin Pan(潘昊霖), Qing Wang(王庆), Qiming Lv(吕崎鸣), Yifei Yan(严轶非), Feng Jin(金锋), Dazhi Hou(侯达之), Lingfei Wang(王凌飞), and Wenbin Wu(吴文彬)
Chin. Phys. B, 2023, 32 (**2**): 027501. DOI: 10.1088/1674-1056/ac67cc

---

Thickness dependence of the magnetic properties of barium ferrite films prepared by pulsed laser deposition

Chengbo Zhao(赵诚博)[1], Bowei Han(韩博纬)[1], Yuchen Zhao(赵宇辰)[2], Yang Sun(孙洋)[2], Lichen Wang(王利晨)[3], Ruoshui Liu(刘若水)[3], Yunzhong Chen(陈允忠)[2], and Dengjing Wang(王登京)[1,†]

[1] *Department of Applied Physics, Wuhan University of Science and Technology, Wuhan* 430065, *China*
[2] *Institute of Physics, Chinese Academy of Sciences, Beijing* 100190, *China*
[3] *CAS Key Laboratory of Magnetic Materials and Devices and Zhejiang Province Key Laboratory of Magnetic Materials and Application Technology, Ningbo Institute of Materials Technology and Engineering, Chinese Academy of Sciences, Ningbo* 315201, *China*

(Received 27 April 2025; revised manuscript received 20 July 2025; accepted manuscript online 1 August 2025)

$BaFe_{12}O_{19}$ (BaM) thin films with thicknesses ranging from 15 nm–200 nm were deposited on Al_2O_3(0001) substrates by pulsed laser deposition (PLD). X-ray diffraction patterns show that a buffer layer with a thickness of nearly 60 nm forms on the substrate, and then a *c*-axis perpendicularly oriented BaM thin film grows on the buffer layer. Atomic force microscopy results indicate that the BaM thin film exhibits a spiral island growth mode on the buffer layer. Magnetic hysteresis loop results confirm that the buffer layer exhibits no significant magnetic anisotropy, while the BaM thin film exhibits perpendicular magnetic anisotropy. The out-of-plane coercivity decreases with increasing BaM thin-film thickness due to the combined effect of grain size growth and lattice strain relaxation. The 200 nm thick film exhibits optimum magnetic properties with $M_s = 319$ emu/cm^3 and $H_c = 1546$ Oe.

Keywords: pulsed laser deposition, barium hexaferrite film, self-made buffer layer, perpendicular magnetic anisotropy, film thickness

PACS: 75.70.–I, 75.60.Ej, 68.37.Ps, 75.30.Gw

DOI: 10.1088/1674-1056/adf6a5 **CSTR:** 32038.14.CPB.adf6a5

1. Introduction

Barium hexagonal ferrite ($BaFe_{12}O_{19}$, BaM) thin films have attracted significant attention as potential materials for high-density recording media and microwave ferrite devices due to their high saturation magnetization, high coercivity, large crystalline anisotropy, high resistivity, large dielectric constant and excellent mechanical hardness and chemical stability.[1,2] Barium hexagonal ferrite belongs to the magnetoplumbite hexagonal crystal system. Its space group is $P63/mmc$ and it has a lattice constant of $a = b = 5.290$ Å and $c = 23.413$ Å (COD database code:1008326).

Several techniques exist for growing BaM thin films, such as sputtering, pulsed laser deposition (PLD), sol–gel processing, chemical vapor deposition and electron beam evaporation, with most aiming to achieve highly oriented growth.[3] PLD offers advantages including composition matching the target material, precise chemical stoichiometry and high growth rate.[4–6] Growth parameters critically influence film properties. Alexander *et al*. reported that insufficient laser energy density leads to the formation of secondary phases in the BaM/Al_2O_3 system.[7] Wei *et al*. demonstrated that elevated substrate temperatures promote highly orientated and well-crystallized BaM films.[8]

In this study, we observe the existence of buffer layer during the initial growth stage of BaM films and investigate the influence of film thickness on the films' magnetic properties.

2. Experiments

The BaM target was commercially purchased with 4 N purity and density of 4.7 g/cm^3. The BaM thin films were deposited on Al_2O_3(0001) substrates by PLD. During deposition, a KrF excimer laser (248 nm) was used, with an energy influence of 674 mJ/cm^2, a repetition rate of 10 Hz, a target-substrate distance of 4 cm, an oxygen pressure of 0.6 Pa, a substrate temperature of 1000 °C and film thicknesses ranging from 15 nm–200 nm.

Structural characterization was performed using a 9 kW high-resolution x-ray diffractometer (HR-XRD), while the film thickness was determined by a step profiler. Surface morphology and magnetic structure of the films were measured by an atomic force microscope (AFM) and a magnetic force microscope (MFM), respectively. The magnetic properties were measured using a superconducting quantum magnetometer MPMS-7 (SQUID 1.9 K–400 K, 0 T–7 T).

3. Results and discussion

The XRD patterns of BaM thin films with different thicknesses are shown in Fig. 1(a). In the XRD patterns of the BaM thin films with thickness from 15nm–60 nm, the diffraction

†Corresponding author. E-mail: wangdengjing@wust.edu.cn

© 2026 Chinese Physical Society and IOP Publishing Ltd. All rights, including for text and data mining, AI training, and similar technologies, are reserved.

peaks are not the BaM (000l) planes, and these diffraction peaks most probably belong to the BaM (116) plane and (2212) plane. However, in the XRD patterns of the 75 nm, 150 nm and 200 nm samples, all significant reflections of the BaM (000l) planes appear in the XRD patterns, which indicates that the BaM film exhibits out-of-plane perpendicular orientation growth.[9] Figure 1(b) reveals the relation between film lattice strain and BaM thin-film thickness. Film lattice strain is calculated by $\Delta d/d_{\text{bulk}}$ ($\Delta d = d_{\text{bulk}} - d_{\text{observed}}$, d is lattice spacing and calculated by Bragg equation $2d \cdot \sin\theta = n \cdot \lambda$, θ is the angle between the incoming ray and the reflected crystal surface, n is the reflection series, n and θ are determined by (008) plane because (008) plane's intensity is the strongest of the (00l) planes, λ is the wavelength and $\lambda = 1.54056$ Å, $d_{\text{bulk}} = 23.413$ Å),[10] and it is found that the lattice strain decreases as the films become thicker, which might be due to the lattice strain relaxation during the film growth. These results demonstrate that as the film thickness increases, a special buffer layer with thickness of nearly 60 nm grows on the Al_2O_3 (0001) substrate, and then c-axis perpendicular orientation BaM thin film grows on the buffer layer. In the initial stage of the thin film growth, the significant lattice mismatch between BaM and Al_2O_3 induces large interfacial stress at the substrate–film interface.[11] To alleviate the lattice strain, a buffer layer with BaM (116) plane forms on the Al_2O_3 (0001) substrate. As the buffer layer thickness increases, the gradual reduction in the angular shift of (116) plane diffraction peaks, as observed in Fig. 1(a), which indicates progressive stress relaxation. When the buffer layer reaches a critical thickness of nearly 60 nm, the lattice strain decreases to an appropriate level. Subsequently, the BaM thin film initiates epitaxial growth with c-axis perpendicular orientation on the buffer layer, and the lattice strain decreases as the growth of the BaM thin films continue. The appearance of the buffer layer is probably intended to alleviate interfacial stress arising from lattice parameter mismatch between the BaM film and Al_2O_3(0001) substrate.

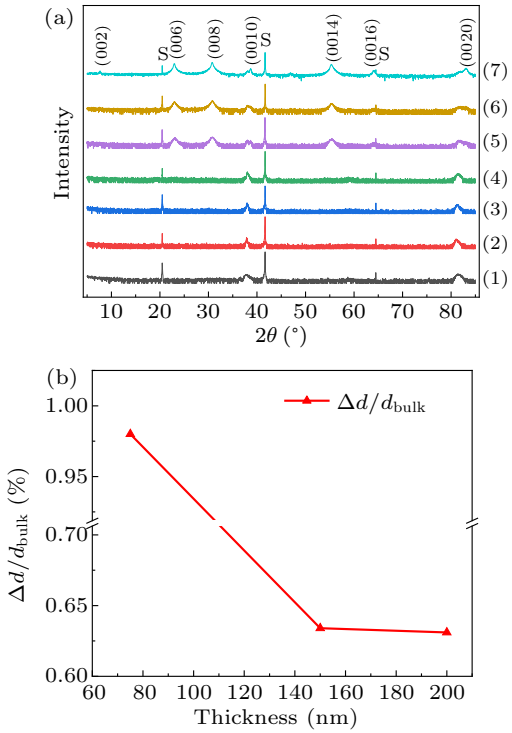


Fig. 1. (a) XRD patterns of different thickness BaM films with (1) 15 nm, (2) 30 nm, (3) 40 nm, (4) 60 nm, (5) 75nm, (6) 150 nm and (7) 200 nm, S: substrate. (b) Relation to lattice strain and BaM thin film thickness.

Figures 2(a)–2(c) show the AFM image of BaM thin films. A significant morphological difference exists between the buffer layer and the BaM thin film. The 150 nm thick film exhibits well-crystallized hexagonal grains, which indicates that the films are grown with c-axis normal to the film plane.[12] The 200 nm thick BaM thin film shows obvious c-axis spiral perpendicular orientation growth mode, and it reveals that the BaM grains nucleate as an island with a screw dislocation in the center and grow by adding BaM to the edge like a spirally rising step.[13] Raistrick also found the same spiral growth mode in $YBa_2Cu_3O_7$/MgO and $YBa_2Cu_3O_7$/$SrTiO_3$ systems.[14] Figure 2(d) is the MFM image of 200 nm BaM thin films. The observed bright and dark contrast image shows domain pattern with cluster-like structure with different out-of-plane magnetic orientations.

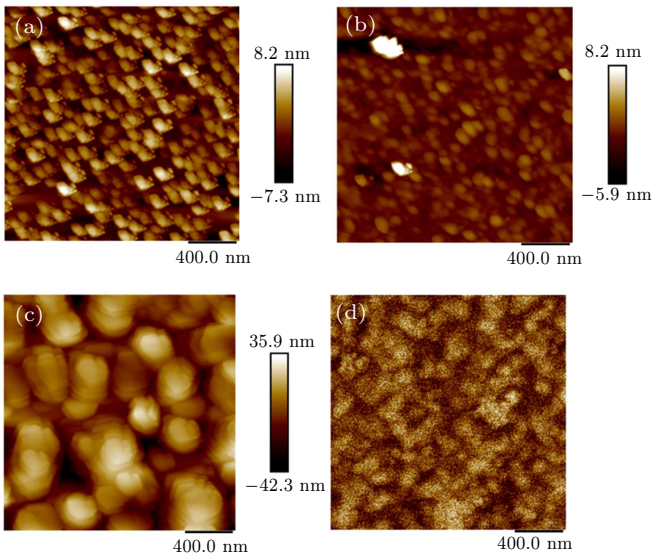


Fig. 2. AFM images of BaM thin films with thicknesses of (a) 15 nm, $Ra = 2.04$ nm, (b) 150 nm, $Ra = 0.893$ nm, and (c) 200 nm, $Ra = 9.29$ nm. (d) MFM image of BaM thin films of 200 nm.

Figures 3(a)–3(d) show out-of-plane and in-plane magnetic hysteresis loops for the BaM thin films. The hysteresis loops were corrected for the substrate's magnetic contribution. In the sample with thickness of 15 nm, the buffer layer exhibits remarkably low coercivity in both in-plane and out-of-plane orientations, and this phenomenon is attributed to the orientation of the (116)-oriented buffer layer. For the samples with thicknesses of 75 nm, 150 nm and 200 nm, the coercivity in out-of-plane orientation is much higher than that in

in-plane orientation, which means that BaM thin films exhibit perpendicular anisotropy.[15] The magnetic anisotropy of BaM originates from its unique crystal structure, wherein two BaM molecules within the unit cell are interconnected through a 180° rotation configuration. This specific arrangement disrupts the symmetry of the BaM crystal unit, thereby inducing magnetic anisotropy.[16] It is observed that the saturation magnetization (M_s) increases with the thickening of the film, which is presumably attributed to the enhanced magnetic properties resulting from the grain growth. The dependence of in-plane and out-of-plane coercivities (H_c) on BaM thin-film thickness is plotted in Fig. 3(e). With increasing BaM thin-film thickness, the grain size expands while the number of crystallites decreases, which results in reduced domain wall pinning resistance. Consequently, the out-of-plane coercivity decreases as the film becomes thicker.[17] As the film thickness increases, the effects from film-substrate interface stress decrease, leading to deteriorated perpendicular growth orientation, and this causes partial orientation towards the in-plane direction, consequently enhancing the in-plane coercivity with film thickening. In the series of BaM thin-film samples, the BaM thin film with 200 nm thickness exhibits optimal magnetic characteristics, achieving the highest saturation magnetization (M_s = 319 emu/cm^3) along with certain coercivity (H_c = 1546 Oe). It can be inferred that as the BaM film becomes thicker during further growth, the saturation magnetization of BaM thin films will increase correspondingly.

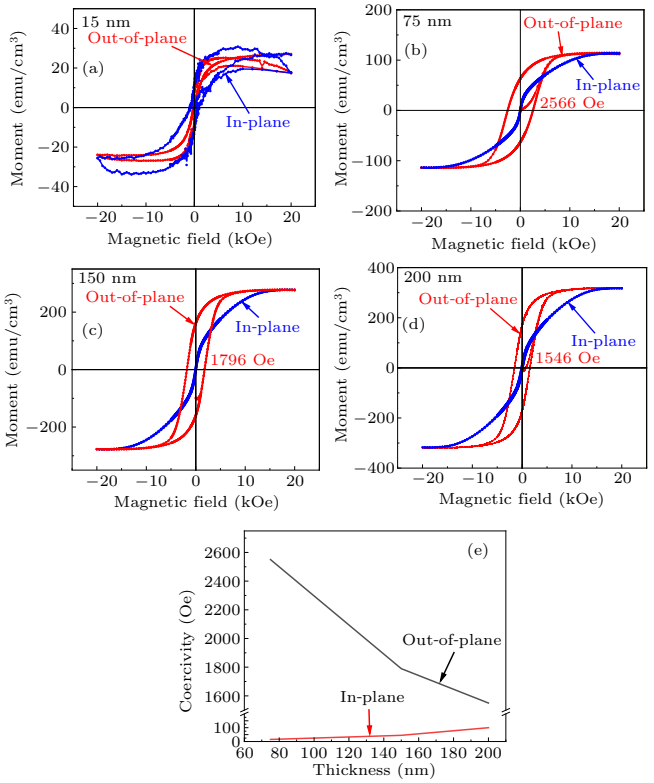


Fig. 3. Out-of-plane and in-plane orientation M–H of BaM thin films with different thicknesses: (a) 15 nm, (b) 75 nm, (c) 150 nm and (d) 200 nm. (e) Change of coercivity versus BaM thin-film thickness.

However, due to the structural constraints inherent in thin-film systems, this value is expected to remain lower than that of bulk BaM materials (M_s = 380 emu/cm^3).[18] In addition, the coercivity will decrease progressively. Furthermore, the inevitable stress relaxation accompanying film thickening will deteriorate the crystallographic orientation, as manifested by diminished texture quality. These degradations prove detrimental to practical applications.

4. Conclusion

The c-axis oriented BaM thin films have been fabricated by the pulsed laser deposition method on the Al_2O_3(0001) substrates. During growth, an approximately 60 nm thick buffer layer initially forms on the substrate, followed by epitaxial growth of c-axis oriented BaM. The buffer layer exhibits negligible coercivity, while the BaM thin film exhibits strong perpendicular magnetic anisotropy due to the almost complete texture with the c-axis orientation normal to the film plane. With increasing thickness of the BaM thin film, the grain size increases accompanied by orientation degradation, leading to enhanced saturation magnetization (M_s), while reducing out-of-plane coercivity and increasing in-plane coercivity. The 200 nm thick film achieves optimum magnetic properties of M_s = 319 emu/cm^3 and H_c = 1546 Oe.

References

[1] Zheng H, Zheng L, Deng J X, Ying Z H and Qin H B 2017 *Mater. Lett.* **190** 263
[2] Chen D, Wang G, Chen Z, Chen Y, Li Y and Liu Y 2017 *Mater. Lett.* **189** 229
[3] Harris V G, Geiler A, Chen Y J, Yoon S D, Wu M Z, Yang A, Chen Z H, He P, Parimi P V, Zuo X, Patton C E, Abe M, Acher O and Vittoria C 2009 *J. Magn. Magn. Mater.* **321** 2035
[4] Yu J, Han W, Abdulsalam Aji Suleiman, Han S Y, Miao N H and Ling F 2024 *Small Methods* **8** 2301282
[5] Li S E, Lin Z F, Hu W, Yan D Y, Chen F C, Bai X B, Zhu B Y, Yuan J, Shi Y G and Jin K 2023 *Chin. Phys. B* **32** 047103
[6] Xiong P Y, Chen F C, Feng Z P, Yang J T, Xia Y D, Yuan Y F, Wang X, Yuan J, Wu Y and Shi J 2023 *Chin. Phys. B* **32** 077402
[7] Yu C, As Sokolov, Kulik P and Harris V G 2020 *J. Alloys Compd.* **814** 152301
[8] Wei X, Zheng H, Chen W, Wu Q, Zheng P, Zheng L and Zhang Y 2020 *Chem. Phys. Lett.* **752** 137541
[9] Song Y Y and Kalarickal S 2003 *J. Appl. Phys.* **94** 5103
[10] Masoudpanah S M, Ebrahimi S A S and Ong C K 2012 *J. Magn. Magn. Mater.* **324** 2654
[11] Shinde S R, Ramesh R, Lofland S E, Bhagat S M, Ogale S B, Sharma R P and Venkatesan T 1998 *Appl. Phys. Lett.* **72** 3443
[12] Shinde S R, Lofland S R, Ganpule C S, Ogale S B, Bhagat S M, Venkatesan T and Ramesh R 1999 *J. Appl. Phys.* **85** 7459
[13] Frank F C 1949 *Discussions of the Faraday Society* **5** 48
[14] Hawley M, Raistrick I D, Beery J G and Houlton R J 1991 *Science* **251** 1587
[15] Zhou K, Chen W, Zheng H, Zheng P, Zheng L, Wu Q and Zhang Y 2021 *Journal of Electronic Materials* **50** 4819
[16] Pullar R C 2012 *Progress in Materials Science* **57** 1191
[17] Fan L N, Zheng H, Shen S Y, Zheng P, Zheng L, Hu J and Zhang Y 2019 *Journal of Electronic Materials* **48** 5717
[18] Valenzuela R 2012 *Physics Research International* **2012** 591839